Resilience Analysis of Cooperative Mission Based on Spatio–Temporal Network Dynamics for Flying Ad Hoc Network

Zhijun Guo , Ying Wang , Yun Sun , Jie Li , Chaoqi Fu , and Jilong Zhong

Abstract—Due to possible disturbances in a conflict environment, the mission performance of flying ad hoc networks (FANET) is highly related to time-varying topology. Currently, the resilience metric is regarded as suitable for evaluating the mission performance of a FANET with time-varying network topology. However, the reported resilience studies contribute little to the theoretical analysis of the impact of the time-varying topology of FANET on a cooperative mission. In this article, an improved resilience analysis method is proposed by defining a new dimension reduction operator, which takes into account the impacts of both isolated and communicated unmanned aerial vehicles. Then, based on random geometry theory, the topological features of FANET are extracted to measure the structure perturbation and recovery. A case study of a joint reconnaissance mission shows that our analysis method is more realistic than the typical method. Our results may be helpful to analyze the resilience of networked dynamic systems and support the more flexible topology control methods design of a FANET.

Index Terms—Cooperative mission, flying ad hoc networks (FANETs), network dynamics, resilience.

NOMENCLATURE

Parameters for the Experiment

Parameter	Descriptions Value.
L	Diameter of the map 300.
R_s	Searching range of each UAV 30.
R_c	Communication range of each UAV 50.
c	Attenuation factor of target information 0.05.
T_1	Time required for full recovery 40.

l_r	Minimum safe distance among UAVs 30.
η	Coupling parameter 0.3.
θ_{GM}	Angle of group motion 0.
σ	Group motion coefficient 0.95.
γ	Random motion coefficient 0.05.
λ_p	Density of the parent PPP 0.01.

I. INTRODUCTION

RECENTLY, the unmanned aerial vehicle (UAV) swarm has been widely used for military and civil activities because of high mobility, low cost, and strong flexibility. To fulfill the system mission, many UAVs work together and interact with others as a UAV swarm through a communication network. A group of drones working in a collective and ad hoc manner forms a flying ad hoc network (FANET) [1]. With a more flexible architecture for communication by multihop links, FANET can support real-time communication for more efficient cooperation between individuals, which is one of the hot issues in the field of wireless communication [2].

The current research interests in FANETs have been focused on the topology architecture, mobility model, and application [3], [4], [5]. However, due to the harsh working environment and complicated mission requirements, the network is required to be self-organized and self-adaptive. Specifically, relying on information interaction, the communication network for a cooperative mission should be designed to adapt to destructive events and restore the network spontaneously. The attribute measuring this dynamic process is usually called resilience. Different from reliability and robustness, resilience characterizes the whole process of a system from interference, damage, and recovery [6]. Hence, resilience will provide a new method for evaluating and improving the cooperative mission performance of a FANET, which is rarely considered by existing works.

Although the current research on resilience has made some promising process, these research works mostly assumed that cooperative interaction links are static or stable, which are quite different from the FANETs. With time-varying spatial network topology, mission performance evaluation of a FANET remains challenging. Based on simulating a certain system behavior and observing mission performance, the reported studies mostly neglect the theoretical analysis for the relation between network structure and mission resilience. [7] Thus, the reported research cannot be expanded for the cooperative mission on FANETs.

To address these limitations, based on the existing models of network space–time dynamics, this article proposes an improved resilience analysis framework of the FANET, which can facilitate us to understand the relation between the time-varying network structure and the specific mission performance. In addition, this article develops the topology model of a FANET by incorporating the influence of node layout and flight mode. The main contributions of our work are as follows.

1) An improved resilience analysis model is proposed to incorporate time-varying network topology.
2) A tractable spatio–temporal network model of the FANET is established based on the Matérn hard-core point process (MHPP) and the reference point group mobility (RGPM) model.
3) The impact of network structure on cooperative mission performance is analyzed, which may facilitate the recovery of a disturbed FANET.

The rest of this article is organized as follows. Section II reviews the related work. In Section III, a FANET spatio–temporal network model is proposed. In Section IV, an improved resilience analysis method for the networked system is proposed. Section V is the theoretical and simulation analysis for a case study. Finally, Section VI concludes this article.

II. RELATED WORKS

For resilience evaluation, the quantitative resilience measurements can be separated into two major categories: general measurement and structural-based measurement [8]. The general measures include deterministic measures and probabilistic measures. Deterministic methods calculate resilience as the cumulative loss of performance. Bruneau et al. [9] defined a deterministic resilience metric as the performance loss. Zobel [10] proposed a resilience triangle paradigm to calculate the resilience after a disturbance event over a long time interval. This paradigm has been applied in several contexts due to its simplicity [11], [12], [13], [14]. To capture the uncertainty associated with system behavior, probabilistic performance-based methods are proposed based on threshold functions. For example, Li and Lence [15] represented resilience as the probability function of failure time and recovery time. Although the general measures are widely applicable, they cannot quantify the impact of structural changes on the system, which is an important issue concerned with the mission resilience of a FANET. To identify the key components of a system, some structural models rely on simulating system behavior and observing performance [16], [17]. For example, Fu et al. [18] developed a cascading model on a mobile spatial network based on simulation, which lacks universal theoretical analysis. However, to characterize the structure mechanism of the resilience, it is necessary to model the collective dynamics of the FANET. Thus, the reported research works are not appropriate for the resilience enhancement of a FANET.

For the collective dynamics on networks, synchronization, i.e., how oscillators linked in a network synchronize with one another in time, has received considerable attention in the past [19], [20]. A great number of theoretical studies have pointed out the conditions when all nodes in the network reach the synchronized state [21]. However, for a specific mission of a FANET, consistent performance may not necessarily mean optimal performance. At one extreme, for instance, the speed of a swarm can be considered consistent even if all UAVs stall. Thus, the synchronization condition cannot keep a cooperative mission resilient. To unveil how the network characteristics can enhance or reduce resilience, Gao et al. [22] proposed a dimensionality reduction method, which can collapse the multidimensional coupled nonlinear equations onto a single universal resilience function. Although the above study provided a universal resilience analysis framework [23], [24], [25], it neglected the inherent capability of UAVs. In fact, a single UAV still contributes to the cooperative mission of the system under self-organization in FANETs. For example, a cooperative search mission for multiple stationary ground targets by a group of UAVs is largely affected by limited sensing capabilities [26]. The above problems make the existing models not applicable to FANETs.

III. SPATIO–TEMPORAL NETWORK MODEL OF A FANET

Due to the temporal and spatial characteristics of the FANET, it is difficult to model the topology of the network. One method is to model the evolution of network topology as a Markov process to quantify the time-varying topology with a stationary distribution [25], [27]. When UAVs are destroyed continuously, the network structure consisting of remaining nodes and edges changes. Meanwhile, the position of each UAV is time-varying with the predefined route. Thus, the network topology of a FANET is related to past time, which means the network evolves under the non-Markovian condition. Hereinafter, the network model is established based on random geometry. If UAVs are modeled as nodes and the communication links between UAVs are modeled as edges, a general network model of a FANET for resilience evaluation is developed as follows (see Fig. 1).

First, to arrange the initial positions of nodes, a node deployment model is determined by the characteristics of the specific mission. Then, on this basis, the mobility model is loaded to determine the location of the nodes on the map at a certain time.

A. Node Deployment Model

We use the Poisson point process (PPP) to model the deployment of locations within a drone group. In general, the point process (PP) theory is the most commonly used in the existing wireless network research, given its mathematical flexibility and theoretical tractability in most cases [28]. The most popular model is the PPP as follows. For a given finite $B \subset \mathbb{R}^d$, if $\Psi(B)$ is the number of points in B, then a PPP Ψ can be characterized by

$$\mathbb{P}\left\{\Psi(B) = n\right\} = \frac{\Lambda(B)^n}{n!}e^{-\Lambda(B)} \tag{1}$$

where intensity measure $\Lambda(B) = \int_B \lambda(x)\mathrm{d}x$ with $\lambda(.)$ is the density of Ψ.

If the dimension $d = 2$, we can use it to model the distribution of the number of UAVs in any independent area B. There are some expansions of PPP to consider the specific modes of node distance in FANET under different missions. The distribution
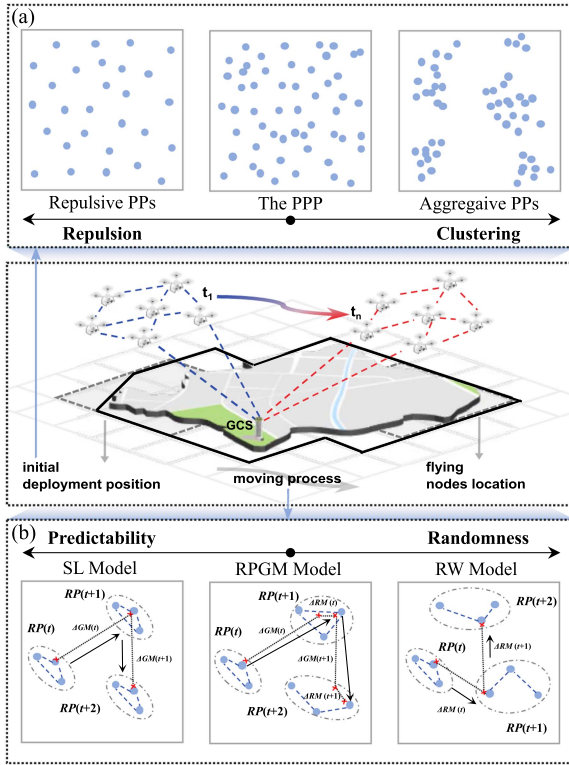
Fig. 1. Composition of the network model of a FANET. (a) Node deployment models with a tendency toward repulsion or clustering. (b) Mobility models with a different tendency toward predictability or randomness.

of different network layouts is shown in Fig. 1(a). For more clustering structures in centralized communication networks, it can be described by the aggregation process, such as the Cox process and the Poisson cluster process. In this article, for FANET we consider the collision-avoiding situation that nodes need to maintain a certain distance to reduce the flight conflict as much as possible. This layout can be described by hard-core process, including MHPP, Poisson hard-core process, etc. They can capture the mutual repulsion between nodes by reducing the density of points. Formally, for a given the minimum safe distance l_r among UAVs, the point density of MHPP λ_{MHPP} is expressed as

$$\lambda_{\text{MHPP}} = \left[1 - e^{-\lambda_p \pi l_r^2} \right] / \pi l_r^2 \tag{2}$$

where λ_p is the density of the parent PPP that is not thinned. Through the above formula, the relative spatial position relation of the nodes over a period of time can be expressed by model parameters such as λ_{MHPP}.

B. Mobility Model

Given the impact of mobility on mission performance, it is critical to select a model close to reality. As shown in Fig. 1(b), the random models, such as the random walk (RW) model, random waypoint (RWP) model, etc. are very easy to analyze with many useful results [29], but the motion mode of FANET is highly controlled with low randomness. In contrast,

the straight line (SL) model [30] is highly predictable, generating the locations based on a predefined route without considering any randomness. However, the flying direction of UAVs may not be always according to the planned route by disturbances in the harsh working environment [31], [32]. The reference point group mobility (RPGM) model can consider both predetermined routes and random directions, which is a combination of the above two models. Thus, we use a reference point group movement model to capture the position of UAVs flying along planned routes in harsh environments and accidents. The locations are updated of UAVs can be expressed according to the following formulas:

$$\overrightarrow{\text{RP}}(t+1) = \overrightarrow{\text{RP}}(t) + \Delta\overrightarrow{\text{GM}}(t) + \Delta\overrightarrow{\text{RM}}(t)$$
$$= \overrightarrow{\text{RP}}(t) + \sigma\overrightarrow{v_{\text{GM}}} + \gamma\overrightarrow{v_{\text{RM}}}(t) \tag{3}$$

where $\text{RP}(t)$ is the location at time t, $\Delta\overrightarrow{\text{GM}}(t)$ is the group motion, $\Delta\overrightarrow{\text{RM}}(t)$ is the random direction disturbance, and $\sigma + \gamma = 1$. When $\sigma = 0$, the above model is equivalent to the RW model, and when $\gamma = 0$ the model is equivalent to the SL model. When the velocity is a constant v, the location can be written as

$$x_{\text{RP}}(t+1) = x_{\text{RP}}(t) + v(\sigma\cos\theta_{\text{GM}} + \gamma\cos\theta_{\text{RM}}) \tag{4}$$
$$y_{\text{RP}}(t+1) = y_{\text{RP}}(t) + v(\sigma\sin\theta_{\text{GM}} + \gamma\sin\theta_{\text{RM}}). \tag{5}$$

Thus, the group motion $\Delta\overrightarrow{\text{GM}}(t)$ is combined with the random direction disturbance $\Delta\overrightarrow{\text{RM}}(t)$ in the RPGM model. Here, the group direction is predefined, which avoids the problem that the flight trajectory of the model does not conform to the actual flight envelope.

C. Network Topology Measure

Some conclusions on the topological characteristics of the above networks are given as follows, which are conducive to the theoretical analysis of resilience in Section IV. In this article, a FANET is modeled as a communication network. If there is a link between two nodes, there is information interaction between the nodes. Affected by signal attenuation, only nodes within the communication range R_c can interact with each other. Specifically, a sufficient and necessary condition for the edge $(u, v) \in G$ is the distance $d(u, v) \leq R_c$. In the following, we give a computation of the probability that a node is an isolated point in a FANET with communication range R_c. Al-Hourani et al. [33] provided an accurate calculation method, but it is too complicated to conduct for practical application. For simplicity, the approximate formulas are given as follows. It is known that if the distribution of nodes in space is a homogeneous PP, the degree of each node D can be expressed by intensity measure as follows:

$$D = \Lambda(S) = \int_S \lambda_{\text{MHPP}}(x)\mathrm{d}x = \lambda_{\text{MHPP}}S(R_c) \tag{6}$$

where S is the communicating area of the node. If the node distribution is PPP, the probability that the node is an isolated point based on the (1) is

$$\text{P}\{\Psi(S(R_c)) = 0\} = e^{-\Lambda(S)}. \tag{7}$$

According to [34], both MHPP and PPP are homogeneous PP. Thus, if we use the PPP with density λ_{MHPP} to approximate the process, we can express the probability that a node is an isolated point P as follows:

$$P\{\Psi(S(R_c)) = 0\} = e^{-\left[1 - e^{-\lambda_p \pi l_r^2}\right]S(R_c)/\pi l_r^2}. \tag{8}$$

The discussion above does not consider the role of mobility in FANET. With the change of nodes' positions, the edges between nodes may change over time according to the interaction mechanism to form a spatio–temporal network topology. Next, we will prove that under our proposed mobility model, the topology can be represented by the above formulas time-independently.

Theorem 1: If Ψ_0 is a homogeneous PP with the density λ, and all nodes move according to the RPGM model, then the moved nodes form a homogeneous PP Ψ with the same density.

Proof: For the RPGM model, the displacement consists of two parts, one is the planned route conforming to the SL model, and the other is the RW model. For both two models above, the flights of nodes are independent identically distributed (i.i.d) and independent of the original positions at time t. Hence, the displaced distances of the RPGM model at every time t are also i.i.d and independent of the original positions. Thus, based on the displacement theorem [34], for a homogeneous PP, the PP after displacement of the RPGM model is a homogeneous PP with the same density λ. □

IV. RESILIENCE ANALYSIS FRAMEWORK FOR THE NETWORK DYNAMICS

In this section, an improved resilience analysis method for a FANET is developed based on the general resilience analysis model. In Section IV-A, we provide some important definitions for resilience analysis and discuss the limitations of the existing model. In Section IV-B, we detail the development of the improved model to capture the impact of a UAV's inherent capability.

A. Preliminaries

To model the resilience of the network, we first introduce the general expression of dynamic process on a multidimensional system. For a networked system with N nodes, the dynamical states $\mathbf{x} = (x_1, \ldots, x_N)^{\text{T}}$ on nodes follow the coupled nonlinear equations:

$$\frac{\mathrm{d}x_i}{\mathrm{d}t} = f(x_i) + \eta_{ij}\sum_{j=1}^{N} a_{ij}g(x_i, x_j) \tag{9}$$

where $f(x_i)$ is the self-dynamics of node i and $g(x_i, x_j)$ is the interactions between node i and node j. The $a_{ij} = 1$ when there is a connection between node i and node j, otherwise $a_{ij} = 0$. The η_{ij} is the adjustable parameter to balance the self-dynamic and the interaction between node j and node i. Generally, it is assumed that the interactions between nodes in the network are homogeneous, i.e., $\eta_{ij} \equiv \eta$ where η is a constant. This assumption is proved to be reasonable and widely used [22].

The above model can be used to model the relationship between the work states of the nodes in a networked system.
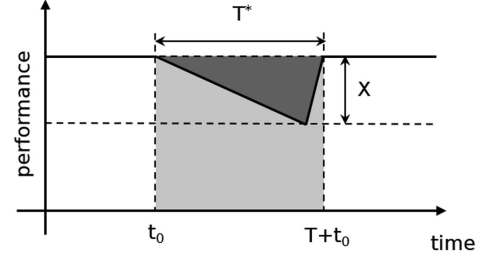

Fig. 2. Interpretation of the resilience triangle.

To model the mission resilience of a FANET, we provide the following definitions.

Definition 1 (Node Performance): Node performance denotes the mission completion status of a node over a period of time. For ease of evaluation, the node performance can be expressed as a ratio compared with the target mission level. In this article, we model node performance as the state variables $\mathbf{x} = (x_1, \ldots, x_N)^{\text{T}}$ of each node. Under a given network structure, the node performances vary from initial values according to the (9). The performance when it no longer varies after a certain period of time is called the steady-state performance.

Definition 2 (Inherent Capability): Inherent capability denotes the performance of a node in a network when it does not interact with other nodes. This parameter is usually determined by the node's own ability to accomplish the mission and does not vary over time, so it is called inherent capability.

Definition 3 (Mission Performance of a FANET): The mission performance of a FANET denotes the performance of all nodes of the network (both isolated and nonisolated points) to accomplish a certain mission while working together. When the $f(\cdot)$ and $g(\cdot)$ of each node are homogeneous, the mission performance of FANET can be represented as the average performance $Z(\mathbf{x})$ of all nodes. $Z(\mathbf{x})$ can be expressed as

$$Z(\mathbf{x}) = \frac{\sum_{i=1}^{N} x_i}{N} \tag{10}$$

where N is the total number of UAVs of the FANET.

Definition 4 (Resilience): Resilience characterizes the whole process of performance from disturbance to recovery. Resilience can be calculated by utilizing performance variations caused by a single disturbance event within a time duration of T^* as follows [10]:

$$R = (T^* - XT/2)/T^* = 1 - XT/2T^* \tag{11}$$

where X is the percentage of performance lost after a disturbance, T is the time required for full recovery, and T^* is a suitably long time interval over which lost performance is determined. As shown in Fig. 2, we assume the original performance of the FANET as $Z(\mathbf{x}_o)$. When the network structure is damaged, the performance will decrease from $Z(\mathbf{x}_o)$ to the steady-state performance $Z(\mathbf{x}_p)$ corresponding to the damaged network. Thus, when fully recovered, the size of the performance lost can be determined, that is, $T^* = T$, the percentage of performance lost X can be calculated as $X = 1 - Z(\mathbf{x}_p)/Z(\mathbf{x}_o)$. In this

situation, the resilience can be calculated as follows:

$$R = 1 - XT/2T^* = \frac{1}{2} + \frac{Z(\mathbf{x_p})}{2Z(\mathbf{x}_o)}. \qquad (12)$$

For ease of evaluation, we provide normalized R_n as follows:

$$R_n = \frac{\frac{1}{2} + \frac{Z(\mathbf{x_p})}{2Z(\mathbf{x}_o)} - \frac{1}{2}}{1 - \frac{1}{2}} = \frac{Z(\mathbf{x_p})}{Z(\mathbf{x}_o)}. \qquad (13)$$

According to (13) for a certain mission, the resilience of a FANET can be expressed as the steady-state performance after failure compared with the original steady-state performance, and the original steady-state performance before disturbance is usually determined as a constant before use. Thus, to evaluate resilience, we will focus on the evaluation of steady-state performance with different network structures. To analyze the mission performance of FANET, we use the linear compression method with a dimension reduction operator to make the high-dimensional dynamics of the cooperative mission computable as proposed in [22]. The definition of dimension reduction operator is as follows.

Definition 5 (Dimension Reduction Operator): If a function aims to reduce the dimension of a system of dynamic equations, it is called a dimension reduction operator. Denote $r(\mathbf{x})$ as a system of equations describing the dynamics of nodes, the operator $Z(\cdot)$ aims to map $r(\mathbf{x})$ to the same effective 1-D equation $r(x)$ as follows:

$$r(\mathbf{x}) \xrightarrow{Z} r(x). \qquad (14)$$

If the network is homogeneous, Gao et al. [22] defined a dimension reduction operator that can compress the dynamics of nodes in a system into a 1-D dynamic equation. Then, the states of all nodes $\mathbf{x} = (x_1, \ldots, x_N)^{\mathrm{T}}$ can be equivalently represented by a 1-D variable x_{eff}, and the incoming degrees $\mathbf{s}^{\mathrm{in}} = (s_1^{\mathrm{in}}, \ldots, s_N^{\mathrm{in}})^{\mathrm{T}}$ of all nodes can be equivalently represented by a 1-D variable β_{eff} as follows:

$$\frac{dx_{\mathrm{eff}}}{dt} = f(x_{\mathrm{eff}}) + \eta \beta_{\mathrm{eff}} g(x_{\mathrm{eff}}, x_{\mathrm{eff}}) \qquad (15)$$

$$\beta_{\mathrm{eff}} = \frac{\mathbf{1}^{\mathrm{T}} \mathbf{A} \mathbf{s}^{\mathrm{in}}}{\mathbf{1}^{\mathrm{T}} \mathbf{A} \mathbf{1}} \qquad (16)$$

$$x_{\mathrm{eff}} = \frac{\mathbf{1}^{\mathrm{T}} \mathbf{A} \mathbf{x}}{\mathbf{1}^{\mathrm{T}} \mathbf{A} \mathbf{1}} \qquad (17)$$

where β_{eff} is the parameter of network structure, x_{eff} is the equivalent state of the all nodes, A is the adjacent matrix of the network, and $\mathbf{1}$ is the unit vector $\mathbf{1} = (1, \ldots, 1)^{\mathrm{T}}$. It is known that when $x_{\mathrm{eff}} = \overline{x}$ is the solution of both $r(x_{\mathrm{eff}}) = \frac{dx_{\mathrm{eff}}}{dt} = 0$ and $\frac{\partial r}{\partial x_{\mathrm{eff}}}\big|_{x_{\mathrm{eff}} = \overline{x}} < 0$, the dynamic process of the system can be guaranteed to be linear stable under the network structure parameter β_{eff}. This method can easily reduce the dimension of a high-dimensional system of equations using a 1-D dynamic equation, thus it can be used to measure the mission performance of a large-scale UAV swarm. However, there are some problems with the above model for the application. First, the variable x_{eff} is the weighted average of performance based on the degree of nodes, that is, the system performance is impacted by other nodes

in proportion to their degrees, which means that the isolated nodes cannot contribute to the cooperative mission. However, affected by dirty environments and constantly situation changing in the mission process, the isolated nodes seem inevitable, but it is still possible to perform under self-organization. Second, the existing model only takes linear stability as the standard of a resilient system, without considering that steady-state performance may also change with changes in network structure.

B. Improved Model

Hereinafter, an improved model is proposed incorporating the inherent capability of the isolated UAV. To measure the mission performance of a FANET, for $\mathbf{x} = (x_1, x_2, \ldots, x_n)^{\mathrm{T}}$ we define dimension reduction operator as follows:

$$Z(\mathbf{x}) = \frac{\mathbf{1}^{\mathrm{T}} \mathbf{x}}{\mathbf{1}^{\mathrm{T}} \mathbf{1}}. \qquad (18)$$

It can be seen that $Z(\mathbf{x})$ is the average performance. Thus, the performance can be expressed by

$$\begin{aligned} Z(\mathbf{x}) &= \frac{\mathbf{1}^{\mathrm{T}} \mathbf{x}}{\mathbf{1}^{\mathrm{T}} \mathbf{1}} \\ &= \left(\sum_{i \in I(t)} x_i + \sum_{i \in C(t)} x_i \right) / |V(t)| \\ &= P(t) Z(\mathbf{x}_{\mathrm{iso}}) + [1 - P(t)] Z(\mathbf{x}_{\mathrm{con}}) \end{aligned} \qquad (19)$$

where $V(t)$ is the total node set at time t, $I(t)$ is the isolated node set at time t, $C(t)$ is the nonisolated node set at time t, and $|\cdot|$ indicates the number of nodes in a certain node set. $\mathbf{x}_{\mathrm{con}}$ is the state vector of the nonisolated node and $\mathbf{x}_{\mathrm{iso}}$ is the state vector of the isolated node. $P(t)$ is the probability of a node to be isolated at time t, which can be expressed as follows:

$$P(t) = |I(t)| / |V(t)| = (1 - |C(t)|) / |V(t)|. \qquad (20)$$

To get steady-state performance, we characterize the dynamics of the system as follows:

$$\frac{dZ(\mathbf{x})}{dt} = P(t) \frac{dZ(\mathbf{x}_{\mathrm{iso}})}{dt} + [1 - P(t)] \frac{dZ(\mathbf{x}_{\mathrm{con}})}{dt}. \qquad (21)$$

The performance of isolated nodes is a constant depends on the inherent capability x_{iso} of the UAV, so $\frac{dZ(\mathbf{x}_{\mathrm{iso}})}{dt} = 0$, thus

$$\frac{dZ(\mathbf{x})}{dt} = [1 - P(t)] \frac{dZ(\mathbf{x}_{\mathrm{con}})}{dt}. \qquad (22)$$

When $P(t) = 1$, all nodes are isolated, so the average steady-state performance $Z(\mathbf{x}) = Z(\mathbf{x}_{\mathrm{iso}}) = x_{\mathrm{iso}}$. When $P(t) \in [0, 1)$, $1 - P(t) > 0$, so the solution $Z(\mathbf{x}_{\mathrm{con}}) = \overline{x}_{\mathrm{con}}$ of both $r(Z(\mathbf{x}_{\mathrm{con}})) = \frac{dZ(\mathbf{x}_{\mathrm{con}})}{dt} = 0$ and $\frac{\partial r}{\partial Z(\mathbf{x}_{\mathrm{con}})}\big|_{Z(\mathbf{x}_{\mathrm{con}}) = \overline{x}_{\mathrm{con}}} < 0$ also satisfies the steady-state condition of $Z(\mathbf{x})$. If the dynamic of nonisolated nodes in the system depends on the (9), the second term of the (9) can be written as follows:

$$\begin{aligned} \sum_{j \in C(t)} a_{ij}(t) g(x_i, x_j) &= s_i^{\mathrm{in}}(t) \frac{\sum_{j \in C(t)} g(x_i, x_j)}{|C(t)|} \\ &= s_i^{\mathrm{in}}(t) Z(g(x_i, \mathbf{x}_{\mathrm{con}})) \end{aligned} \qquad (23)$$

where $s_i^{\text{in}}(t)$ is the incoming degree of node i at time t. Based on the mean field theory, $Z(g(x_i, \mathbf{x}_{\text{con}})) \approx g(x_i, Z(\mathbf{x}_{\text{con}}))$, (9) can be written as follows:

$$\frac{\mathrm{d}x_i}{\mathrm{d}t} = f(x_i) + \eta s_i^{\text{in}}(t)g(x_i, Z(\mathbf{x}_{\text{con}})). \qquad (24)$$

For all nonisolated nodes, the dynamic equations can be expressed as follows:

$$\frac{\mathrm{d}\mathbf{x}_{\text{con}}}{\mathrm{d}t} = f(\mathbf{x}_{\text{con}}) + \eta \mathbf{s}_{\text{con}}^{\text{in}}(t) \circ g(\mathbf{x}_{\text{con}}, Z(\mathbf{x}_{\text{con}})) \qquad (25)$$

where $\mathbf{s}_{\text{con}}^{\text{in}}(t)$ is the incoming degrees of all nonisolated nodes and the operator $\circ$ represents the Hadamard product. Applying the operator in (18), based on the mean-field theory $\frac{\mathrm{d}Z(\mathbf{x}_{\text{con}})}{\mathrm{d}t} = 0$ can be rewritten as follows:

$$\frac{\mathrm{d}Z(\mathbf{x}_{\text{con}})}{\mathrm{d}t} = Z(f(\mathbf{x}_{\text{con}})) + Z(\eta \mathbf{s}_{\text{con}}^{\text{in}}(t) \circ g(\mathbf{x}_{\text{con}}, Z(\mathbf{x}_{\text{con}})))$$
$$\approx f(Z(\mathbf{x}_{\text{con}})) + \eta Z(\mathbf{s}_{\text{con}}^{\text{in}}(t))g(Z(\mathbf{x}_{\text{con}}), Z(\mathbf{x}_{\text{con}})). \qquad (26)$$

Let $x_{\text{con}} = Z(\mathbf{x}_{\text{con}})$ and $\beta_{\text{con}}(t) = Z(\mathbf{s}_{\text{con}}^{\text{in}}(t))$, (26) can be rewritten as follows:

$$\frac{\mathrm{d}x_{\text{con}}}{\mathrm{d}t} = [f(x_{\text{con}}) + \eta\beta_{\text{con}}g(x_{\text{con}}, x_{\text{con}})]. \qquad (27)$$

Given the average degree of isolated nodes is 0, the average degree $\beta(t)$ of all nodes at time t is calculated as follows:

$$\beta(t) = Z(\mathbf{s}_{\text{iso}}^{\text{in}}(t)) + Z(\mathbf{s}_{\text{con}}^{\text{in}}(t)) = [1 - P(t)]\beta_{\text{con}}(t) \qquad (28)$$

therefore, the 1-D equation of the nonisolated nodes is written in terms of x_{con} as follows:

$$\frac{\mathrm{d}x_{\text{con}}}{\mathrm{d}t} = f(x_{\text{con}}) + \eta\beta(t)g(x_{\text{con}}, x_{\text{con}})/[1 - P(t)]. \qquad (29)$$

Thus, when the solution $Z(\mathbf{x}_{\text{con}}) = \bar{x}_{\text{con}}$ satisfies $r(Z(\mathbf{x}_{\text{con}})) = \frac{\mathrm{d}Z(\mathbf{x}_{\text{con}})}{\mathrm{d}t} = 0$ and $\left.\frac{\partial r}{\partial Z(\mathbf{x}_{\text{con}})}\right|_{Z(\mathbf{x}_{\text{con}})=\bar{x}_{\text{con}}} < 0$, the steady-state performance $\bar{x}$ can be written as follows:

$$\bar{x} = Z(\mathbf{x}) = P(t)x_{\text{iso}} + [1 - P(t)]\bar{x}_{\text{con}}. \qquad (30)$$

V. CASE STUDY

To illustrate the advantages of our improved model, we take a cooperative reconnaissance mission of a UAV swarm as a case for theoretical analysis and simulation in this section. Section V-A details the mission background and the parameters settings. Section V-B presents a theoretical study under this mission to validate the proposed model. In Section V-C, we compare the simulation results with the theoretical results of two models discussed in Section V-B. In Section V-D, we discuss the impact of the structure disturbance and recovery in the case.

A. Mission Background

To verify our model, we conduct simulation experiments on the following mission. We study the joint reconnaissance mission of fixed targets on a specific battlefield by a group of UAVs with limited sensing and communication capabilities similar with the case proposed in [26]. By observing each patch of the

---

Algorithm 1: Simulation of a Joint Reconnaissance Mission for a UAV Swarm.

Input: The inherent parameters of the system;
Output: The mission performance of getting the true distribution of the targets;

1: Set the targets on the battlefield map $\mathbf{T}$ and the locations of all UAVs based on MHPP model;
2: Initialize the probability map $\mathbf{P}^i$ of each UAV i, $i = 1, 2, \ldots, N_t$;
3: Initialize the network topology of the system based on locations;
4: **for** $t \leftarrow 1$ to t_{total} **do**
5:   **for** $i \leftarrow 1$ to the number N_t of UAVs **do**
6:     Update the location (x_i, y_i) of UAV i based on RPGM model, $\forall(x, y) \in L \times L$;
7:     **if** t is the attack time point **then**
8:       Update the network topology after perturbation caused by the attack strategy;
9:     **if** t is the recovery time point **then**
10:       Update the recovered network topology;
11:   **for** $i \leftarrow 1$ to the number N_t of UAVs **do**
12:     **for** $j \leftarrow (i + 1)$ to N_t of UAVs **do**
13:       Calculate the Euclidean distance d_{ij} between UAV i and other UAV j;
14:       Delete or create the edge e_{ij} when $d_{ij} > R_c$ or $d_{ij} \leq R_c$;
15:   **for** $i \leftarrow 1$ to the number N_t of UAVs **do**
16:     Update $\mathbf{P}_{(m,n),t}^i$ with targets information in the searching region $(x_i - R_s, x_i + R_s) \times (y_i - R_s, y_i + R_s)$;
17:     Update $\mathbf{P}_t^i$ with exchanged information from neighbors based on Eq.(32);
18: Calculate the mission performance $O(\text{t})$.

---

map, each UAV obtains 0 (no target is detected) or 1 (a target is detected) as detection results. For each UAV, a probability map is reserved as the observation of the whole battlefield at a time step. The targets on the battlefield are uniformly distributed. Thus, the average mission performance $O(t)$ at time t can be represented by the probability of finding targets as follows:

$$O(t) = 1 - \frac{\sum_i \sum_{xy} |p_{xy}^i - s_{xy}|}{NL^2} \qquad (31)$$

where p_{xy}^i is the probability map element of UAV i on the location (x, y), s_{xy} is the actual map element on the same location, N is the number of UAVs, and L is the battlefield diameter.

Since the searching range of each UAV is less than the battlefield diameter L, the target searching highly depends on information exchange via the FANET. As shown in Fig. 3(a), each UAV can only communicate with agents within its communication range and shares target information through links at a certain time t, and the green square represents the targets. The information between UAVs is updated and fused cooperatively
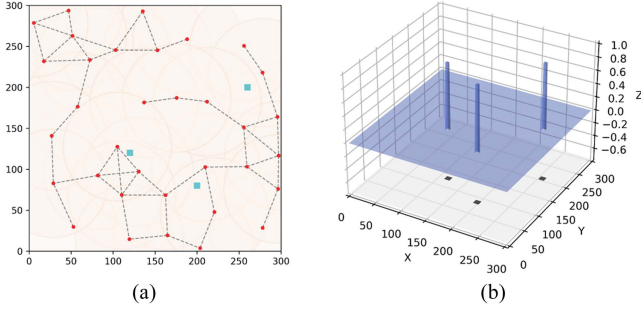
Fig. 3. Joint reconnaissance mission of UAVs via a FANET. (a) Communication network topology and the target distribution on the battlefield at a certain moment. (b) Convergence of the probability map.

Fig. 4. Theoretical result of the existing model and the improved model. (a) Existing model. (b) Improved model.

until probability maps converge to reflect the actual target distribution. Fig. 3(b) shows the convergent probability maps of all UAVs, which can reflect the actual distribution of targets.

B. Theoretical Analysis

If we define the performance x_i of each node as the proportion of target information obtained in the entire map, for nonisolated nodes in a swarm, the dynamics of information propagation in cooperative reconnaissance is as follows:

$$\frac{\mathrm{d}x_i}{\mathrm{d}t} = -cx_i + \eta \sum_{j=1}^{N} a_{ij}(1 - x_i)x_j \qquad (32)$$

where c is the factor describing the attenuation of self-obtained target information when interacting with other nodes and the second term represents the information interaction mechanism between each UAV. When the UAV has got enough information, it will not need to receive target information from other UAVs. In addition, we define that the planned route is a horizontal scanning and the targets are distributed based on the MHPP model on the map. Thus, the x_{iso} can be estimated by the ratio of the searching area to the map area per unit time as follows:

$$x_{\mathrm{iso}} = v(2R_s + 1)/vL = \frac{(2R_s + 1)}{L} \qquad (33)$$

where R_s is the searching range and L is the diameter of the map.

Based on (15), the theoretical results of the existing model is

$$\begin{cases} \bar{x}_0 = 0, \text{ if } 0 < \beta_{\mathrm{eff}} < \frac{1}{6} \\ \bar{x}_1 = 1 - \frac{c}{\eta\beta_{\mathrm{eff}}}, \text{ if } \beta_{\mathrm{eff}} \geq \frac{1}{6} \end{cases} . \qquad (34)$$

While the theoretical result of our model is

$$\bar{x}_1 = P(t)\frac{(2R_s + 1)}{L} + (1 - P(t))\left(1 - \frac{c}{\eta\beta(t)}\right). \qquad (35)$$

Based on (6), the average degree of each node in FANET $\beta(t)$ can be approximately expressed by the distribution density of nodes and communicating area as follows:

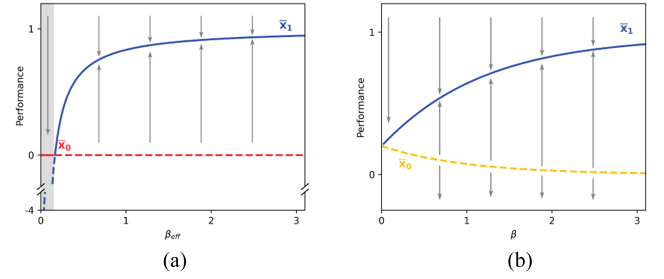$$\beta(t) = \Lambda(S(t)) = \lambda_{\mathrm{MHPP}}(t)(2R_c + 1)^2. \qquad (36)$$

Then, (35) can be written as follows:

$$\bar{x}_1 = e^{-\beta(t)}\frac{(2R_s + 1)}{L} + \left(1 - e^{-\beta(t)}\right)\left(1 - \frac{\eta}{c\beta(t)}\right)$$

$$= e^{-\lambda_{\mathrm{MHPP}}(t)(2R_c+1)^2}\frac{(2R_s + 1)}{L} + \left(1 - e^{-\lambda_{\mathrm{MHPP}}(t)(2R_c+1)^2}\right)$$

$$\left(1 - \frac{\eta}{c\lambda_{\mathrm{MHPP}}(t)(2R_c + 1)^2}\right). \qquad (37)$$

The theoretical results of the two models are shown in Fig. 4. Fig. 4(a) shows the prediction results of the existing model, and $\bar{x}_0$ and $\bar{x}_1$ represent two solutions, respectively. The solid line represents a stable performance and the dotted line represents that the solution cannot be stable. When $\beta_{\mathrm{eff}} \leq \frac{1}{6}$, it can be seen that the predicted performance of the system is constantly equal to 0, which means that the analysis scheme cannot describe the performance level of the damaged system. In comparison, the result of the improved model is shown in Fig. 4(b). When the structure parameter $\beta \leq \frac{1}{6}$, the performance still decreases with the decrease of β. If $\beta = 0$, then $\bar{x}_1 = x_{\mathrm{iso}}$. The results show that the performance of isolated nodes in the system can be fully considered in our proposed model.

C. Simulation Analysis

In this section, we present the simulation results of resilience analysis under different parameters based on the algorithm mentioned above. The simulation process is shown in Algorithm 1. The experiment parameter setting is given in the Nomenclature. In addition, we apply standard parameter values for R_s = 30/patches, R_c = 50/patches, and T_1 = 40/ticks, unless otherwise specified. All the results of simulations are averages obtained over 30 simulations unless otherwise specified. To evaluate the performance changes from damage to recovery, hereinafter we clarify two types of performance changes. We simulate the disturbances to FANET in reality by setting a structural and functional perturbation separately. Fig. 5 shows the change of the mission performance when 30% of the nodes are disturbed functionally and structurally, respectively. The functional perturbation refers to that the performance is reduced without the network structure change, for example, clearing some target location records. On the contrary, the structural perturbation will destroy the network structure without changing the information obtained by nodes. Our model indicates that
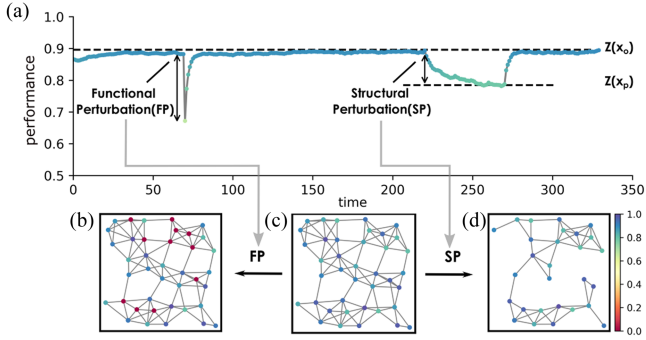
Fig. 5. Two kinds of perturbation in a network. (a) Performance under different perturbations. The network structure and nodes performance at different time steps: (b) after the functional perturbation, (c) before the functional perturbation and after the recovery, and (d) after the structural perturbation.
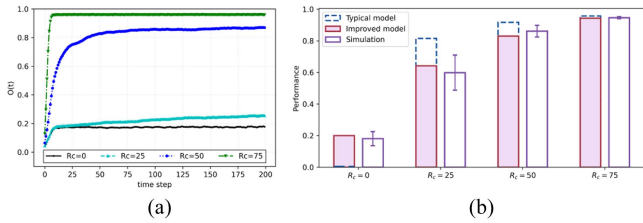

Fig. 6. Results and comparisons between simulation and theory under different R_c. (a) $O(t)$ under different R_c. (b) Comparisons between the improved model and the typical model.

Fig. 7. Results and comparisons between simulation and theory under different R_s. (a) $O(t)$ under different R_s. (b) Comparisons between the improved model and the typical model.

Fig. 8. Results of simulation with different failure nodes proportion. (a) Changes of $O(t)$ with different q. (b) $\beta(t)$ under different q. (c) Performance as a function of β.

the performance of the resilient system can recover without external intervention when only functional perturbation occurs. However, when structural perturbation occurs, the steady-state performance changes with the β changing. Thus, to recover the performance after structural perturbation, it is necessary to restore the network structure.

To compare the results under different communication circumstances, we study the impact of communication range R_c. As shown in Fig. 6(a), there are different steady performances for different R_c, which is determined by the network dynamics. With increasing range, the performance of the network gradually increases. For $R_s \neq 0$, the probability of finding targets $O(t)$ is not equal to 0 when $R_c = 0$. This result indicates that a UAV can contribute to the mission independently. As shown in Fig. 6(b), we compare simulation results with the values of the two models under different R_c. It is found that when $R_c = 0$, the predicted value of the typical model is 0, which is significantly less than the actual value. However, the result of the improved model is approximate to the actual value. In all cases, the improved model provided the results more in agreement with the simulation results.

To illustrate the impact of the sensing capability of a single UAV on mission performance, we assume that all UAVs flew on the mission independently, i.e., all R_c of UAVs are set to the same value as 0. As shown in Fig. 7(a), the performance of the system increases linearly with the R_s increases, which is in line with the prediction of the (35). As shown in Fig. 7(b), with the
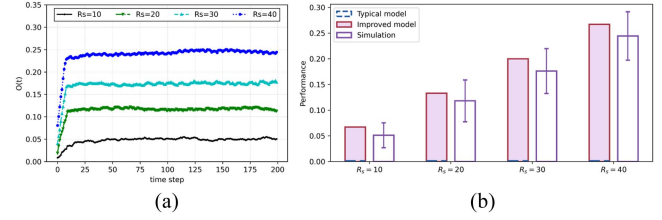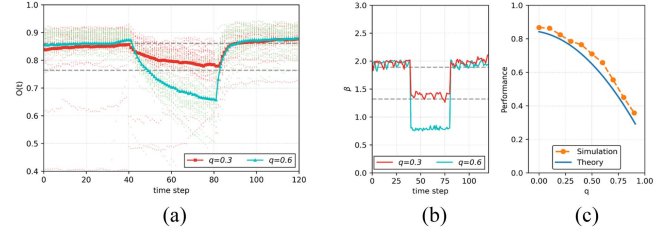
increase of R_s, the improved model can correctly predict the trend of performance. On the contrary, the typical model cannot model the effect of the change of R_s. The results of the improved model are generally greater than the simulation results, which is due to the error caused by approximation and randomness in numerical simulation.

To study the impact of structural perturbation on mission performance, we use the resilience measure proposed above. As shown in Fig. 8(a), it can be found that when structural perturbation occurs, the mission performance tends to the new steady performance as predicted (the dotted line indicates the theoretical value). As shown in Fig. 8(b), with the failure nodes proportion q increasing, the structure parameter β decreases proportionally in the corresponding time interval. In Fig. 8(c), the relation between the mission performance and the perturbation is shown. We note that the results decrease with the increase of q in both theoretical analysis and simulation. It is found that the numerical simulation results are consistent with the improved model's theoretical values. The results indicate that our model can quantitatively characterize the relation between network structure and mission performance, which is difficult for most existing models.

From the above results, it can be seen that we can recover performance by recovering the structural parameter β. According to (36), β is related to the density of nodes and communication range R_c. Thus, there are two schemes for system structure restoration: 1) the R-scheme—in this scheme, we consider that restore the network structure by improving the communication range R_c of UAV through energy control and 2) the N-scheme—in this scheme, we restore the number of nodes in the network to the original number by supplementing redundant UAVs. When $q = 0.3$, the effects of the above recovery schemes are shown in
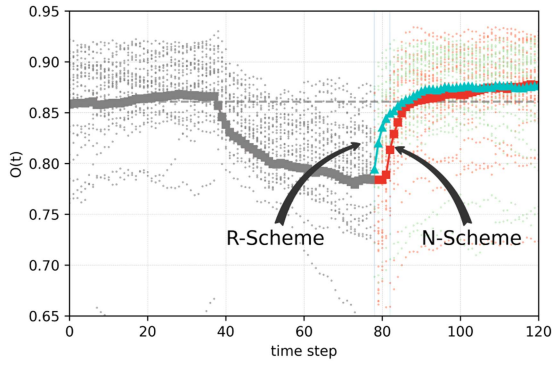
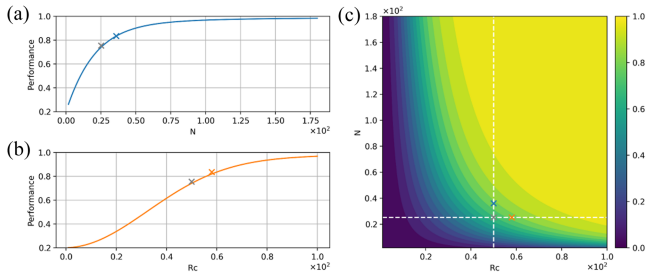Fig. 9.　Two kinds of recovery schemes for the structural perturbation.

Fig. 10.　Comparisons between R-scheme and N-scheme for recovery. (a) Plot of performance as a function of N. (b) Plot of performance as a function of R_c. (c) Phase diagram for performance with different N and R_c.

Fig. 9. We carry out the R-scheme and N-scheme at $t = 78$ and $t = 82$, respectively. It is found that both schemes can restore the mission performance to the level before the perturbation.

Furthermore, we provide discussions on the selection of recovery schemes. To compare the effects of the above schemes, the curves for varying R_c and N are separately shown in Fig. 10(a) and (b). Under the above case, compared with the communication range increasing, the performance improves more rapidly with the supplements of nodes. The phase diagram for the mission performance with the parameter changes is shown in Fig. 10(c). Although both recovery schemes can recover performance, when R_c is large (about more than 30), the N-scheme facilitates more rapid performance recovery, and vice versa when N is large (about more than 30), the R-scheme can be a better scheme. The above example shows how our model helps to develop the strategy of system recovery.

VI. CONCLUSION

Due to the disturbance and the change in the relative position between UAVs, the topology of the FANET is constantly changing when the system flew on the mission. However, the performance of the system is determined by the dynamic process on the network affected by the topology. Thus, it is difficult to analyze the resilience of a cooperative mission on FANETs. Recent studies have proposed resilience analysis methods considering spatio–temporal dynamics, neglecting the impact of the inherent capability of UAVs on the mission performance. Based on the existing model, we propose an improved model incorporating the inherent capability and the topology change to characterize

the resilience. Compared with the typical models, the proposed model is more in agreement with the simulation results.

The case study shows that the relation between structure changes and the performance of a resilient system can be characterized and analyzed quantitatively by our model. It is found that the mission performance largely depends on the communication range and the number of UAVs. For the UAV removal caused by an attack, our analysis framework reflects the trend that the performance decreases with the proportion of UAV loss increasing. In addition, by the proposed method in this article, we can compare the effects of different schemes for restoring the network structure, which may facilitate rapid recovery of mission performance.

In this article, the FANET we focus on is homogeneous, i.e., each UAV in the system plays the same role. However, the scenarios of heterogeneous units jointly executing tasks began to appear in reality recently. We may extend our work to the analysis of the heterogeneous FANET. In addition, the UAV swarm may tend to be more self-organized with intelligent technology in the future. We plan to investigate the intelligent topology control methods based on the mechanism of FANET resilience in future research.

REFERENCES

[1] A. Srivastava and J. Prakash, "Future FANET with application and enabling techniques: Anatomization and sustainability issues," *Comput. Sci. Rev.*, vol. 39, 2021, Art. no. 100359.

[2] İ. Bekmezci, O. K. Sahingoz, and Ş. Temel, "Flying Ad-Hoc networks (FANETs): A survey," *Ad Hoc Networks*, vol. 11, pp. 1254–1270, 2013.

[3] A. Chriki, H. Touati, H. Snoussi, and F. Kamoun, "FANET: Communication, mobility models and security issues," *Comput. Netw.*, vol. 163, 2019, Art. no. 106877.

[4] D. Shumeye Lakew, U. Sa'ad, N.-N. Dao, W. Na, and S. Cho, "Routing in flying ad hoc networks: A comprehensive survey," *IEEE Commun. Surveys Tut.*, vol. 22, no. 2, pp. 1071–1120, Apr.-Jun. 2020.

[5] J. Guo et al., "STMTO: A smart and trust multi-UAV task offloading system," *Inf. Sci.*, vol. 573, pp. 519–40, 2021.

[6] D. D. Woods, "Four concepts for resilience and the implications for the future of resilience engineering," *Rel. Eng. Syst. Saf.*, vol. 141, pp. 5–9, 2015.

[7] J. Friginal, D. de Andrés, J.-C. Ruiz, and M. Martínez, "REFRAHN: A resilience evaluation framework for ad hoc routing protocols," *Comput. Netw.*, vol. 82, pp. 114–34, 2015.

[8] S. Hosseini, K. Barker, and J. E. Ramirez-Marquez, "A review of definitions and measures of system resilience," *Rel. Eng. Syst. Saf.*, vol. 145, pp. 47–61, 2016.

[9] M. Bruneau et al., "A framework to quantitatively assess and enhance the science the seismic resilience of communities," *Earthq. Spectra*, vol. 19, pp. 733–752, 2003.

[10] C. W. Zobel, "Representing perceived tradeoffs in defining disaster resilience," *Decis. Support Syst.*, vol. 50, pp. 394–403, 2011.

[11] J. Chen, J. Liu, Q. Peng, and Y. Yin, "Resilience assessment of an urban rail transit network: A case study of Chengdu subway," *Physica A: Stat. Mechanics Appl.*, vol. 586, 2021, Art. no. 126517.

[12] C. W. Zobel and L. Khansa, "Characterizing multi-event disaster resilience," *Comput. Operations Res.*, vol. 42, pp. 83–94, 2014.

[13] T. M. Adams, K. R. Bekkem, and E. J. Toledo-Durán, "Freight resilience measures," *J. Transp Eng.*, vol. 138, pp. 1403–1409, 2012.

[14] H.-W. Wang et al., "Evaluation and prediction of transportation resilience under extreme weather events: A diffusion graph convolutional approach," *Transp. Res. Part C: Emerg. Technol.*, vol. 115, 2020, Art. no. 102619.

[15] Y. Li and B.J. Lence, "Estimating resilience for water resources systems," *Water Resour. Res.*, vol. 43, 2007, Art. no. W07422.

[16] G. Bai, Y. Li, Y. Fang, Y.-A. Zhang, and J. Tao, "Network approach for resilience evaluation of a UAV swarm by considering communication limits," *Rel. Eng. Syst. Saf.*, vol. 193, 2020, Art. no. 106602.

[17] X. Fu and Y. Yang, "Modeling and analyzing cascading failures for Internet of Things," *Inf. Sci.*, vol. 545, pp. 753–770, 2021.

[18] X. Fu, W. Li, and Y. Yang, "Exploring the impact of node mobility on cascading failures in spatial networks," *Inf. Sci.*, vol. 576, pp. 140–156, 2021.

[19] A. Barabási, *Network Science*. Cambridge, U.K.: Cambridge Univ. Press, 2016.

[20] H. Su and X. Wang, *Pinning Control of Complex Networked Systems*. Berlin, Germany: Springer, 2013.

[21] L. Pecora and T. Carroll, "Master stability functions for synchronized coupled systems," *Phys. Rev. Lett.*, vol. 80, 1998, Art. no. 2109.

[22] J. Gao, B. Barzel, and A.-L. Barabási, "Universal resilience patterns in complex networks," *Nature*, vol. 530, pp. 307–312, 2016.

[23] Y. Zhang, C. Shao, S. He, and J. Gao, "Resilience centrality in complex networks," *Phys. Rev. E*, vol. 101, 2020, Art. no. 022304.

[24] H. Sanhedrai, J. Gao, A. Bashan, M. Schwartz, S. Havlin, and B. Barzel, "Reviving a failed network through microscopic interventions," *Nature Phys.*, vol. 18, pp. 338–349, 2022.

[25] X. Lu, H. Wang, and Y. Deng, "Evaluating the robustness of temporal networks considering spatiality of connections," *Chaos, Solitons Fractals*, vol. 78, pp. 176–184, 2015.

[26] J. Hu, L. Xie, K.-Y. Lum, and J. Xu, "Multiagent information fusion and cooperative control in target search," *IEEE Trans. Control Syst. Technol.*, vol. 21, no. 4, pp. 1223–1235, Jul. 2013.

[27] S. Scellato, I. Leontiadis, C. Mascolo, P. Basu, and M. Zafer, "Evaluating temporal robustness of mobile networks," *IEEE Trans. Mobile Comput.*, vol. 12, no. 1, pp. 105–117, Jan. 2013.

[28] Y. Hmamouche, M. Benjillali, S. Saoudi, H. Yanikomeroglu, and M. D. Renzo, "New trends in stochastic geometry for wireless networks: A tutorial and survey," *Proc. IEEE*, vol. 109, no. 7, pp. 1200–1252, Jul. 2021.

[29] T. Camp, J. Boleng, and V. Davies, "A survey of mobility models for ad hoc network research," *Wireless Commun. Mobile Comput.*, vol. 2, pp. 483–502, 2002.

[30] M. Banagar and H. S. Dhillon, "Performance characterization of canonical mobility models in drone cellular networks," *IEEE Trans. Wireless Commun.*, vol. 19, no. 7, pp. 4994–5009, Jul. 2020.

[31] O. Bouachir, A. Abrassart, F. Garcia, and N. Larrieu, "A mobility model for UAV ad hoc network," in *Proc. Int. Conf. Unmanned Aircr. Syst.*, 2014, pp. 383–388.

[32] H. Wang, H. Zhao, J. Zhang, D. Ma, J. Li, and J. Wei, "Survey on unmanned aerial vehicle networks: A cyber physical system perspective," *IEEE Commun. Surveys Tut.*, vol. 22, no. 2, pp. 1027–1070, Apr.-Jun. 2020.

[33] A. Al-Hourani, R. J. Evans, and S. Kandeepan, "Nearest neighbor distance distribution in hard-core point processes," *IEEE Commun. Lett.*, vol. 20, no. 9, pp. 1872–1875, Sep. 2016.

[34] F. Baccelli, "Stochastic geometry and wireless networks: Volume I Theory," *Found. Trends Netw.*, vol. 3, pp. 249–449, 2009.